Up and down cascades: Three-dimensional magnetic field model

E. M. Blanter,[1,2] M. G. Shnirman,[1,2] and J. L. Le Mouël[2]
[1]*International Institute of Earthquake Prediction Theory and Mathematical Geophysics, Warshavskoye sh 79, korp 2, Moscow 113556, Russia*
[2]*Institut de Physique du Globe de Paris, 4, place Jussieu, 75252 Paris Cedex 05, France*

(Received 12 November 2001; published 17 June 2002)

In our previous works we already have proposed a two-dimensional model of geodynamo. Now we use the same approach to build a three-dimensional self-excited geodynamo model that generates a large scale magnetic field from whatever small initial field, using the up and down cascade effects of a multiscale turbulent system of cyclones. The multiscale system of turbulent cyclones evolves in six domains of an equatorial cylindrical layer of the core. The appearance of new cyclones is realized by two cascades: a turbulent direct cascade and an inverse cascade of coupling of similar cyclones. The interaction between the different domains is effected through a direct cascade parameter which is essential for the statistics of the long-life symmetry breaking. Generation of the secondary magnetic field results from the interaction of the components of the primary magnetic field with the turbulent cyclones. The amplification of the magnetic field is due to the transfer of energy from the turbulent helical motion to the generated magnetic field. The model demonstrates a phase transition through the parameter characterizing this energy transfer. In the supercritical domain we obtain long-term intervals of constant polarity (chrons) and quick reversals; relevant time constants agree with paleomagnetic observations. Possible application of the model to the study of the geometrical structure of the geomagnetic field (and briefly other planetary fields) is discussed.

DOI: 10.1103/PhysRevE.65.061105 PACS number(s): 05.40.−a, 91.25.Cw, 47.65.+a

I. INTRODUCTION

The magnetic field of the Earth is a natural phenomenon that has been widely used in practical human life from very ancient times, but whose origin and mechanism are not completely clear up to now. Our knowledge of the properties of the geomagnetic field comes from paleomagnetic data (not very precise) and recent observations that are precise enough, but encompass a very short period in the geological time scale. Some features of the field are however well established. At the Earth's surface it is for the main part, most of the time, equivalent to the magnetic field of a dipole located at the center of the Earth whose axis is not far from the axis of the Earth's rotation. Taken in average over a few thousands years, this dipole is aligned along the rotation axis. Paleomagnetic data show that the dipole changes its polarity from time to time, completing the so-called polarity reversals. The durations of reversals (of the order of 10^3 years) are short compared with the durations of constant polarity, referred to as chrons (from 10^5 to 10^6 years). The amplitude of the magnetic field exhibits strong temporal variations during chrons, but never remains close to zero for a long time (in the geological sense).

It is generally believed that the geomagnetic field is the result of a dynamo process in the metallic fluid core of the planet. A lot of theoretical works and numerical simulations have been devoted to the construction of models of this process. Let us quote only three of the different approaches considered in recent times.

First, simple analog models, such as the disk dynamo [1–3], leading to a few coupled differential equations, have been considered.

Second, there have been several attempts to model the effect on a magnetic field of a small scale turbulent motion in the core fluid. In some models, in particular, Refs. [4–7], the effect of a turbulent small scale motion on a large scale magnetic field is estimated through a mean field theory and is shown to generate a large scale secondary magnetic field (α effect). This mechanism is characterized by a scalar field α (in the core), which is generally given *a priori* in the so-called nearly axisymmetric dynamo models [8–13]. Recently, stochastic geodynamo models based on the mean field approach also appeared [14].

A third approach consists in the building of impressive numerical codes to solve directly the relevant magnetohydrodynamic equations, which has given rather spectacular results (see, e.g., [15] for a review). Nevertheless, in all the models constructed so far [16–24], the numerical values given to the parameters are not relevant for the core. For example, the Ekman number, which measures the importance of viscous effects, is never taken smaller than 10^{-5} whereas the value relevant for the core is probably 10^{-15}. So, hyperviscosity is introduced in most of the models. The same procedure is most often applied to thermal and magnetic diffusivities (whose ratios to the kinematic viscosity are measured by the Prandtl and magnetic Prandtl number), introducing the so-called hyperdiffusivities. This procedure, however essential in the numerical work, to enhance the dissipation of higher spectral components of the fields, which cannot be resolved numerically, is hard to justify theoretically (considering that some kind of turbulent viscosity in the core reduces the gap, but this viscosity would probably be highly anisotropic [25]). And unfortunately the effect of hyperviscosity or hyperdiffusivities on the larger scale solution is difficult to access (e.g., [18,26,27]).

It is interesting to note that most of the numerical models produced in the last few years succeeded (even with Ekman numbers close to 0.1) in producing an external field dominated by an axial dipolar component, and even, in some cases, reversals of the dipoles (although computations are not carried out long enough to allow any statistics). This would lead to an optimistic view about the models capturing essential features of the geomagnetic field generation, should not the generation mechanisms in the models be so different: "some models generate the magnetic field by chaotic motions inside the cylinder tangent to the inner core (e.g., [16]), others by chaotic motions outside this cylinder [21,22]; some propose a giant α effect in columnar structures comparable to nonmagnetic convection rolls (e.g., [28,29] or [20]); some stress the role of boundary layers (e.g., [30]) in the field generation while others artificially suppress them [19,21,22,31])." Busse's statement "the impression currently in vogue that the problem of the origin of the Earth's magnetic field had been solved is overly optimistic" [31] still holds even now. This is not, of course, to question the importance of numerical codes that meet an increasing success; but the present status of the geodynamo problem does not preclude efforts along different lines [3,14].

The application of hierarchical cascade models to the simulation of the magnetic field started with [32], where the idea of the α effect was combined with an inverse cascade of the small scale turbulence. The model developed in [33] produced long-life breaks of symmetry in a basically symmetric multiscale turbulent model because of the coworking of both direct and inverse cascades. Interacting with a constant primary magnetic field, the system of cyclones of the model generates a secondary magnetic field; the breaks of symmetry of the cyclones system give rise to periods of time when the secondary magnetic field keeps a constant sign, which are the chrons of the model. In [34], the model was made similar to an autoexcited dynamo; there is no longer any preexisting primary field. Models [33,34] give rather realistic pictures of the evolution of the geomagnetic field (on geological time scales), but they are rather two dimensional (2D) in nature (although with a hint of 3D), and no localization is possible inside the dynamo volume. We will not repeat further here the general considerations concerning the geodynamo and α effect [33,34], but will make a step forward from a two-dimensional model of the turbulent motion in the liquid core to a three-dimensional model of multiscale turbulence.

The present work uses the principle of the two-sides cascade model of [33]; we apply it to a three-dimensional system of three-dimensional cyclones, although again discreet in space. A three-dimensional additional magnetic field is generated at each time by the interaction of the magnetic field existing at this time and the multiscale system of cyclones. The evolution of the cyclones has features similar to those encountered in the previous models [33,34], but the mechanism of the interaction of the cyclones with the magnetic field is different. Each component (in a Cartesian frame) of the local magnetic field interacts with the system of cyclones and makes a contribution to the two other components of the field. The system can become autoexcited, and we can investigate which kind of condition determines the amplification process, the dipolar geometry, and the characteristics of the evolution of the generated magnetic field, which displays long-life chrons and quick reversals.

Physical assumptions entering the general construction of the model are presented in Sec. II. Section III contains a step-by-step description of the evolution of the system of cyclones. The evolution of the magnetic field is described in Sec. IV. The choice of the parameters of the modeling and the results are presented in Sec. V. Possible extensions of the model and the physical sense of the obtained results are discussed in Sec. VI.

II. BASIC ASSUMPTIONS

In order to construct a model of a self-excited three-dimensional geodynamo we adopt some assumptions about the processes taking place in the liquid core of the Earth, and make some simplifications concerning the geometrical properties of the volume where the geomagnetic field is generated. Some of our simplifications may be strong, and the discretization used in the model is rather rough; nevertheless, we try to construct quite a general model where all effects and results are easily understandable.

As a basis of our model we use again a multiscale system of cyclones governed by both a usual direct turbulent cascade and an inverse cascade due to electromagnetic coupling; in [33] this system was shown to produce amplification and polarity reversals of the secondary magnetic field. The present three-dimensional construction naturally realizes a self-exited dynamo model as in [34], but now each component of the magnetic field interacts with the system of cyclones in such a way as to produce a secondary magnetic field contributing to the two components orthogonal to itself, and so on.

We consider that we construct our model in an equatorial symmetric band of the core; this allows us to neglect the spherical form of the Earth while conserving axial symmetry with respect to the axis of rotation. The main idea of the space discretization consists in subdividing the considered layer into several domains in each of which it is possible to choose a local basis of coordinates with the X axis normal to the core surface, the Y axis tangential to the core surface, and the Z axis parallel to the Earth's rotation axis. This approach allows us to consider each of these domains separately and to neglect in each of them the change of the normal to the core surface. The global magnetic field is then built as the vector sum of the local magnetic fields generated in the same way in each of the local domains.

The idea of discretization is transferred from the space volume to the type of cyclones. Although the orientation of 3D cyclones in a 3D space may be quite arbitrary, we consider only 12 basic kinds of cyclones determined by the orientation of the motion with respect to the local basis axes. The continuous evolution of the state of cyclones is represented by two discrete states, as in [33], and the stochastic transition from the first to the second state is also as in [33].

The model we develop in the following uses a rather abstract and schematic representation of a developed turbulence in the core and also an abstract mechanism of magnetic field generation. A comparison with detailed magnetohydrodynamics (MHD) computations as the ones recalled in the

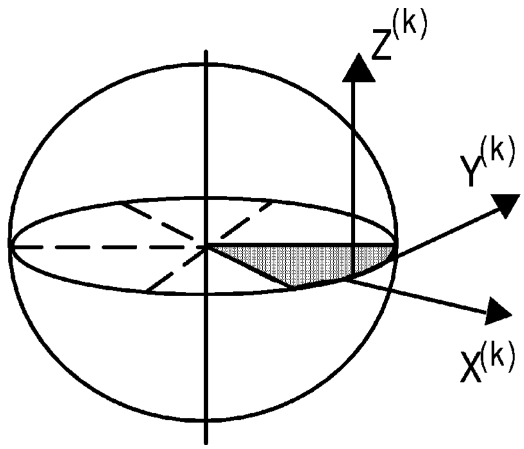

FIG. 1. Local basis in a domain of the Earth.

Introduction is not straightforward, although the basic idea is the same: fluid motion (here a schematic multiscale helical motion with up and down cascades) and a magnetic field (which we represent in each domain by a vector **H** (H_x, H_y, H_z), the largest scale component of an actually multiscale field) can interact in such a way as to give long constant polarity time intervals and reversals of the resulting field. Magnetic field generation and electromagnetic interaction of cyclones are images of, respectively, the induction equation and the Lorentz force. One can also say that we build a mechanism for transferring energy from the cyclonic motion to the magnetic field, the transfer depending on the scale of the cyclone. We intend to make the correspondence between MHD and our abstract model clearer in a dedicated paper.

A. System of interacting domains

The considered volume of liquid core of the Earth is subdivided in six domains defined by their sections in the equatorial plane (Fig. 1). As said above, each domain has a local coordinates system $(X^{(k)}, Y^{(k)}, Z^{(k)})$ with the $Z^{(k)}$ axis parallel to the Earth's rotation axis, the X axis normal to the surface of the core and the Y axis tangential to this surface (Fig. 1). We characterize the magnetic field in each domain k by a vector $\boldsymbol{H}^{(k)}$ (referred to below as the magnetic field vector of kth domain), which is decomposed into the vector sum of its three orthogonal components in the local basis:

$$\boldsymbol{H}^{(k)} = \boldsymbol{H}_x^{(k)} + \boldsymbol{H}_y^{(k)} + \boldsymbol{H}_z^{(k)}, \tag{1}$$

where $k = 1, \ldots, 6$ is the index of the domain, and coordinates of $\boldsymbol{H}_x^{(k)}$ $\boldsymbol{H}_y^{(k)}$ and $\boldsymbol{H}_z^{(k)}$ in the local basis (of kth domain) are $(H_x^k, 0, 0)$, $(0, H_y^k, 0)$, and $(0, 0, H_z^k)$, respectively.

The magnetic field $\boldsymbol{H_k}$ of a domain is, of course, not confined in this domain. Let P be a point of the rotation axis at distance d from the Earth's center, and consider the total field $\boldsymbol{H}$ (resulting from the contribution of the 6 domains) at P.

Choosing a global Cartesian frame X, Y, Z (Z is again along the rotation axis), H_x, H_y, H_z being the components of $\boldsymbol{H}$, it becomes

$$H_x = \sum_{k=1}^{6} (H_x^{(k)} h_{xx}^{(k)} + H_y^{(k)} h_{xy}^{(k)}),$$

$$H_y = \sum_{k=1}^{6} (H_x^{(k)} h_{yx}^{(k)} + H_y^{(k)} h_{yy}^{(k)}), \tag{2}$$

$$H_z = \sum_{k=1}^{6} H_z^{(k)}.$$

$h_{xx}^{(k)}$ is a factor determining essentially the projection of the local axis $X^{(k)}$ on the global X axis; $h_{xy}^{(k)}$ corresponds to the projection of the $Y^{(k)}$ onto X; $h_{yx}^{(k)}$ to the projection of $X^{(k)}$ on Y; $h_{yy}^{(k)}$ to the projection of $Y^{(k)}$ on Y. For symmetry reasons the h_{ij}^k depend on d the same way for all k.

The evolution of $\boldsymbol{H}$ will be considered in the following and compared to the observations.

Remark. The number of sectors, n, has been chosen equal to six as the result of a compromise: not to make the computations too lengthy while conserving as much as possible the symmetries of the equatorial cylindrical layer. The value of this compromise has been tentatively checked (not however by full computations): the behavior of the model is not significantly changed for $n > 6$, and it would remain qualitatively unchanged for $n = 4$.

B. Turbulence and cyclones

A multiscale turbulence is assumed to exist in the liquid core of the Earth. Interaction of localized vortices has been studied in [35–39]. The study of the MHD of a helical flow can be found in [40]; fully developed MHD turbulence has been considered in [41,42]. We adopt here a more phenomenological point of view. The turbulence generates a multiscale system of cyclones in each domain. Due to the axial symmetry of the Earth we postulate the same statistical properties of the turbulence in all six domains. Each cyclone is determined by its direction of motion and its orientation of rotation. In order to simplify the model, only cyclones directed along the basis axes are considered: in each domain the *motion* of a cyclone is parallel to one of the three axes of the local basis $(X^{(k)}, Y^{(k)}, Z^{(k)})$; we denote cyclones moving along X, Y, Z as Λ_x, Λ_y, and Λ_z, respectively. The motion of a cyclone can be positive or negative with respect to the direction of the axis; the *rotation* of the cyclone will be considered positive or negative depending on the sign of the rotation with respect to its translation (right-handed orientation is taken as positive) (Fig. 2). Eventually, 12 kinds of cyclones (4×3) are considered in each domain. The size of a cyclone is determined by its scale level $l = 1, \ldots, L$ as follows:

$$s(l) = s_0 \rho^l, \tag{3}$$

where $\rho > 1$; the size of a cyclone grows with its level l.

The temporal evolution of cyclones is schematically expressed by two possible states: *strong* or *weak*. A cyclone always appears in the strong state and can be disintegrated (disappear) only in the weak state.

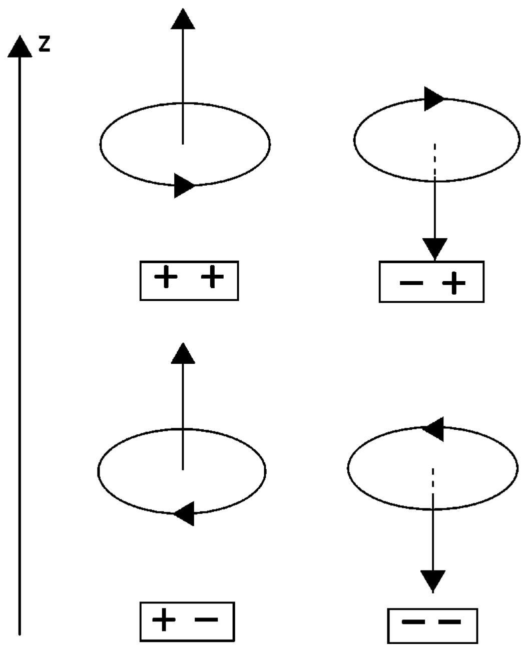

FIG. 2. Different kinds of cyclones relevant to the Z axis of the local basis.

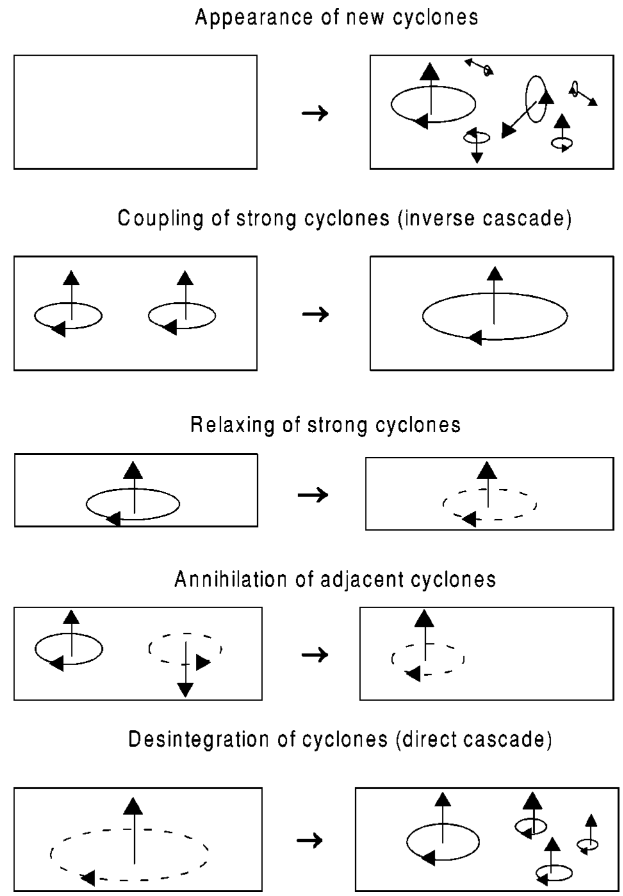

FIG. 3. Different steps of the evolution of cyclones. Strong cyclones are plotted by solid lines; weak cyclones are plotted by dashed lines. Arrows show directions of the cyclone's motion and rotation.

The evolution of the system of cyclones is governed by five independent processes (Fig. 3, see also [33]).

(1) Turbulent appearance of new strong cyclones at all levels of the system (direct cascade).

(2) Coupling of strong cyclones of the same kind at level l and generation of a new cyclone of the same kind at higher level $l+1$ (inverse cascade).

(3) Relaxing of strong cyclones: the strong state of cyclones changes into the weak state.

(4) Annihilation of close cyclones of different kinds: strong cyclones become weak, weak cyclones disappear.

(5) Disintegration of weak cyclones and generation of new cyclones of the same kind at all inferior levels (direct cascade).

C. Interactions between the system of cyclones and the magnetic field

An helical motion in the core produces an electric current when a primary magnetic field is present. This current, in turn, generates a secondary magnetic field that adds to the primary one. This is the mechanism working in the α effect where, however, only small scale helical motions are considered. The extension to our schematic multiscale flow is not straightforward; but we stick, in the present paper, to a rather abstract formalism. As the magnetic field vectors $\boldsymbol{H}^{(k)}$ are discretized along the three orthogonal components, it is easy to describe the interaction between turbulent cyclones and $\boldsymbol{H}^{(k)}$, as well as the secondary magnetic field generation. Basic ideas and assumptions are as follows.

(1) Cyclones in the kth domain interact only with the local magnetic field vectors $\boldsymbol{H}_n^{(k)}$ $(n=x,y,z)$, and the secondary magnetic field generated is also added to the local magnetic field of this domain. Any influence of other domains is neglected at this step.

(2) Cyclones with motion along the rth axis $\Lambda_r(l)$ $(r=x,y,z)$ interact with the two components $\boldsymbol{H}_n^{(k)}$ orthogonal to the r axis $(n\neq r, n=x,y,z)$.

(3) The generated secondary magnetic field vector, $\widetilde{\boldsymbol{H}}_m^{(k)}$, is orthogonal to both the direction of the cyclone motion r and the vector component $\boldsymbol{H}_n^{(k)}$ this cyclone interacts with $(m,n,r=x,y,z;\ m\neq n,\ m\neq r,\ n\neq r)$.

(4) The amplitude of the generated secondary magnetic field vector component, $|\widetilde{H}_m^{(k)}|$, grows with the size of the cyclone $\Lambda_r(l)$ [determined by its level l, Eq. (3)] and the amplitude of the primary magnetic field vector component $H_n^{(k)}$.

(5) The direction of the generated secondary magnetic field vector component $\widetilde{H}_m^{(k)}$ is positive or negative depending on the kind of cyclone $\Lambda_r(l)$ and the direction of the primary magnetic field vector component $H_n^{(k)}$ (Fig. 4).

So, each cyclone interacts with two of the three components of the local magnetic field in the considered domain and contributes to the two components of the secondary magnetic field orthogonal to its direction of motion.

In turn, as in [34], the existing local magnetic field reacts on the intensity of coupling, relaxing and annihilation, due to

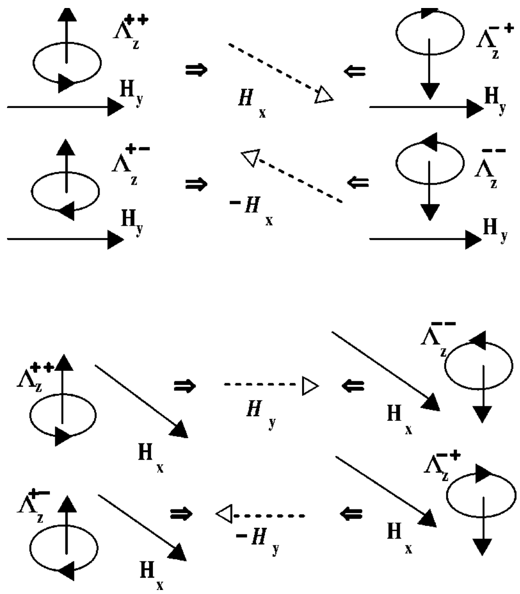

FIG. 4. Interaction between vector components $\boldsymbol{H}_r^{(k)}$ ($r = x,y,z$) of the local magnetic field with cyclones of different kinds.

the effect of the electromagnetic attraction or repulsion of the electric currents associated with the cyclones.

III. EVOLUTION OF CYCLONES

In this section we give a detailed description of all of the steps of the cyclones evolution. The main principles are the same as in [33]; there are, however, some changes due to the three-dimensional approach.

As all six domains are similar, we describe the system for one particular local domain without indicating its number, dropping index (k); however, we do keep in mind that the local magnetic field, basis vectors, and cyclones are different in the different domains. Constant parameters, on the contrary, are generally assumed to be the same for all the domains (otherwise it will be specified).

A. Turbulent appearance

Cyclones randomly appear at all levels of the system because of the multiscale turbulence flow (Fig. 3). The full developed turbulence is assumed to be isotropic at low scales $l \leqslant L_0$, but to present anisotropy at higher scales $L_0 < l \leqslant L$; turbulence at high scales is oriented along the Earth's rotation axis. The intensity of turbulent appearance of cyclones is

$$\varepsilon_x(l) = \varepsilon_y(l) = \varepsilon_z(l) = a_0 \eta^l, \quad l < L_0,$$
$$\varepsilon_x(l) = \varepsilon_y(l) = 0, \quad L_0 \leqslant l \leqslant L, \tag{4}$$
$$\varepsilon_z(l) = a_z \eta_z^l, \quad L_0 \leqslant l \leqslant L.$$

Continuity at $l = L_0$ implies

$$a_z = a_0 \left(\frac{\eta}{\eta_z} \right)^{L_0}. \tag{5}$$

Cyclones of kind Λ_i at level l appear with intensity $\varepsilon_i(l)$ defined by Eq. (4), (here we denote by i the axis x, y, or z).

B. Coupling of strong cyclones of the same kind

Appearance of a new cyclone at the higher level $l+1$ from two strong cyclones of the same kind at level l is referred to as a *coupling* (Fig. 3). Two kinds of coupling are assumed: coupling of pairs of *neighbor* cyclones, coupling of *isolated* cyclones. We denote the intensity of coupling as $\alpha_r(l,t)$ for adjacent cyclones and $\gamma_r(l,t)$ for isolated cyclones (r denotes the direction x, y, or z, l is a scale level, t is the time). The intensity of coupling is in both cases taken proportional to the square of the electric current density, density which is itself proportional to the corresponding component of the present magnetic field; so the intensities of coupling depend on the square of the local magnetic field components as follows.

1. Coupling of neighbors

$$\alpha_x(l,t) = \{1 - \exp[-\alpha_0(H_y^2 + H_z^2)]\}\mu^l,$$
$$\alpha_y(l,t) = \{1 - \exp[-\alpha_0(H_x^2 + H_z^2)]\}\mu^l, \tag{6}$$
$$\alpha_z(l,t) = \{1 - \exp[-\alpha_0(H_x^2 + H_y^2)]\}\mu^l.$$

The scaling parameter μ $(0 < \mu < 1)$ expresses a lower probability of coupling for larger cyclones; α_0 is a given dimensional constant.

2. Coupling of isolated cyclones

$$\gamma_x(l,t) = \{1 - \exp[-\gamma_0(H_y^2 + H_z^2)]\}g^l, \tag{7}$$

$$\gamma_y(l,t) = \{1 - \exp[-\gamma_0(H_x^2 + H_z^2)]\}g^l, \tag{8}$$

$$\gamma_z(l,t) = \{1 - \exp[-\gamma_0(H_x^2 + H_y^2)]\}g^l. \tag{9}$$

The scaling parameter g has the same meaning as μ in Eq. (6), γ_0 is a given dimensional constant.

We assume that the new cyclones generated by the coupling appear first at free places (without neighbors): the appearence of a new isolated cyclone is favored with respect to the appearence of a new pair of adjacent cyclones [33].

C. Relaxing of strong cyclones

Strong cyclones are *relaxing* into the weak state (Fig. 3) with intensity

$$D(l) = D_0 \delta^l, \tag{10}$$

where $\delta < 1$ is a scaling parameter that expresses the increasing stability of cyclones with level.

D. Annihilation of adjacent cyclones

We assume that in the case two adjacent cyclones attract each other due to the electromagnetic force, but cannot couple because of their different directions of motion, they destroy one another with a probability proportional to the square of the corresponding component of the magnetic field. This process is referred to as the *annihilation* (Fig. 3). Annihilation means transition to the weak state for a strong cyclone, and disappearance for a weak cyclone. Just as the intensity of coupling, the intensity of annihilation is written as follows:

$$S_x(l,t)=\{1-\exp[-S_0(H_y^2+H_z^2)]\}\sigma^l,$$
$$S_y(l,t)=\{1-\exp[-S_0(H_x^2+H_z^2)]\}\sigma^l, \tag{11}$$
$$S_z(l,t)=\{1-\exp[-S_0(H_x^2+H_y^2)]\}\sigma^l.$$

E. Disintegration of weak cyclones (direct cascade)

Weak cyclones disintegrate with the following intensity:

$$\beta(l)=\beta_0 b^l. \tag{12}$$

As a result, new cyclones of the same kind appear at all lower levels of the system (Fig. 3) with the intensity

$$\kappa(\Lambda,l,t)=1-\exp\left\{-F_0\sum_{\lambda=l+1}^{L}[B(\Lambda,\lambda,t)+w(B_+(\Lambda,\lambda,t)+B_-(\Lambda,\lambda,t))]\phi^{\lambda-l}\right\}, \tag{13}$$

where $B(\Lambda,\lambda,t)$ is the density of disintegrated cyclones of type Λ at level λ at time t. The number of disintegrated cyclones $B(\Lambda,\lambda,t)N(\lambda)$ [variable $N(\lambda)$ is the total possible number of cyclones coexisting at level λ] is a Poissonian random variable of parameter $\beta(l)W(\Lambda,\lambda,t-1)$, where $W(\Lambda,\lambda,t)$ denotes the number of weak cyclones of type Λ at level λ at time $t-1$. The contributions of cyclones disintegrating in the two neighbor domains [$k-1$ and $k+1$(mod 6)], denoted $B_+(\Lambda,\lambda,t)$ and $B_-(\Lambda,\lambda,t)$, are taken into account with weight w. Interaction of cyclones in different domains is realized via the just described process of disintegration and controlled by the parameter w that is very essential for the synchronous evolution of the model.

IV. EVOLUTION OF THE LOCAL MAGNETIC FIELDS

We consider the different processes contributing to the evolution of the magnetic field, and model them in terms of losses and gains of the local magnetic field vectors $\boldsymbol{H}^{(k)}$. Let us consider a vector component $\boldsymbol{H}_r^{(k)}$ ($r=x$, y or z) in the kth local domain and describe which processes contribute to its evolution in the time interval $[t,t+1]$.

Dissipation. We assume that the magnetic field strength permanently decreases because of Ohmic dissipation, denoted as Δ, proportional to the actual strength of the magnetic field itself. The dissipation being isotropic, we assume that all components of the magnetic field are multiplied by $(1-\Delta)$ for each time step of the modeling.

Losses due to the interaction with cyclones. The magnetic field component H_r interacts with cyclones whose directions of motion are along the local axes $m\neq r$, with a contribution to the magnetic field components $q\neq r$, $q\neq m$. This interaction requires a transfer of energy from the existing magnetic field; therefore we assume a loss of intensity of the component H_r proportional to both H_r and a global characteristics of the cyclones, $\tilde{D}_r$. This characteristic $\tilde{D}_r$ is the sum of characteristics $U(\Lambda)$ for all the kinds of cyclones Λ interacting with the magnetic field component H_r: it gives

$$\tilde{D}_x(t)=\sum_{\Lambda_y}U(\Lambda_y,t)+\sum_{\Lambda_z}U(\Lambda_z,t),$$
$$\tilde{D}_y(t)=\sum_{\Lambda_x}U(\Lambda_x,t)+\sum_{\Lambda_z}U(\Lambda_z,t), \tag{14}$$
$$\tilde{D}_z(t)=\sum_{\Lambda_x}U(\Lambda_x,t)+\sum_{\Lambda_y}U(\Lambda_y,t).$$

We write $U(\Lambda)$ as a weighted sum of the numbers of cyclones of kind Λ and level l, the weight of the cyclones increasing with their scale level. The difference between contributions of strong and weak cyclones is taken into account through two parameters h^+ and h^-, it is

$$U(\Lambda,t)=\sum_{l=1}^{L}[h^+N^+(\Lambda,l,t)+h^-N^-(\Lambda,l,t)]\chi^l. \tag{15}$$

The scaling parameter $\chi>1$ leads to a larger contribution of high scale levels; $N^+(\Lambda,l,t)$ and $N^-(\Lambda,l,t)$ denote, respectively, the number of strong and weak cyclones of type Λ and level l, weighting constants h^+ and h^- are normalized in order to avoid difficulties with high-level systems ($L\to\infty$):

$$h^+=h_0^+\left(\sum_{l=1}^{L}\chi^l\right)^{-1}, \tag{16}$$

$$h^-=h_0^-\left(\sum_{l=1}^{L}\chi^l\right)^{-1}. \tag{17}$$

Gains due to the interaction with cyclones. There are two additive contributions A_i^j and A_j^i to the component H_r because of the interaction of the two components H_i and H_j, respectively, ($i\neq j\neq r$) with cyclones. The additive contribution A_i^j may be positive or negative depending on the orientation of the cyclone with respect to the ith axis and on the sign of the component H_j. We determine the sign of the contribution A_i^j from a matrix Γ of ±1. The component $\Gamma_i^{\Lambda_j}$ gives the sign of the contribution to the component r ($r\neq i\neq j$) resulting from the interaction of a cyclone of kind Λ_j with the ith component of the local magnetic field (Fig. 4). Just as the loss $\tilde{D}$ described above, the additive contribution A_i^j is proportional to the sum $U(\Lambda_j)$ defined by Eq. (15), which counts the cyclones of kind Λ_j characterized by a motion directed along jth axis.

The additive term A_i^j contains two contributions: a transfer of energy from H_i to H_r due to the interaction of H_i with cyclones, proportional to H_i, and a transfer of kinetic energy from the motion of cyclones to H_r. The second contribution also depends on H_i because the transfer of energy from the motion is the result of the interaction between the magnetic field and cyclones, and it is zero when the intensity of the magnetic field is zero. For large values of the magnetic field intensity, the contribution A_i^j to the magnetic field cannot increase faster than H_i (otherwise an unlimited growth of the magnetic energy would be possible); a saturation mechanism is necessary. On the other hand, when the magnetic field is weak, the increase of the field energy is mainly governed by the transfer of kinetic energy from the system of cyclones. This last condition suggests the way the kinetic energy transferred from the cyclones to the magnetic field can depend on H_i: we take it proportional to $\sqrt{H_i}$ (this choice is rather arbitrary). Finally we assume the following expression for A_i^j:

$$A_i^j = \sum_{\Lambda_j} U(\Lambda_j, t)\sqrt{kH_i^2(t) + H_0|H_i(t)|}\,\Gamma_i^{\Lambda_j}, \tag{18}$$

where $0<k<1$ is a dimensionless constant that governs the loss of energy during the transfer from the component H_i to H_r; H_0 is a constant determining the transfer of the kinetic energy of cyclones to the magnetic field and has the same dimension as H_i. When the magnetic field intensity H_i is strong enough the quantity below the square root in Eq. (18) is determined by its first term kH_i^2, and therefore the contribution A_i^j is proportional to the H_i, as said above.

Finally the expression of the variation of the local magnetic field components from t to $t+1$ gives

$$\begin{aligned} H_x(t+1) &= H_x(t)(1-\Delta)[1-\tilde{D}_x(t)] + A_y^z + A_z^y, \\ H_y(t+1) &= H_y(t)(1-\Delta)[1-\tilde{D}_y(t)] + A_x^z + A_z^x, \\ H_z(t+1) &= H_z(t)(1-\Delta)[1-\tilde{D}_z(t)] + A_x^y + A_y^x. \end{aligned} \tag{19}$$

V. RESULTS

In previous sections we have written the equations governing the evolution of our model. The results presented below are obtained from a random simulation of these equations; in other words we are considering a stochastic process whose mean values are governed by the proposed equations.

The detailed registration of the evolution of the magnetic field of the Earth covers less than 150 years. However the evolution of the amplitude of, essentially, the axial dipolar part of the field can be reconstructed from paleomagnetic data, which are in fact time averaged. In order to better compare our model with paleomagnetic data we also average in time the magnetic field vector $\boldsymbol{H}$: we look at the evolution of the vector $\boldsymbol{H}(t_k)$ defined as the mean value of the vector $\boldsymbol{H}(t)$ over the time interval $(t_k - T, t_k)$. In the simulations below $T=100$.

There are two features of the geomagnetic field that we wish to reproduce in our model. First, the main part of the real geomagnetic field is its axial dipolar component; in terms of our model, the Z component of the global magnetic field has to be much larger than the other two components. Second, the real geomagnetic field has long periods of constant polarity while its changes of polarity are relatively fast; we expect such a behavior for the magnetic field $\boldsymbol{H}$ of our model.

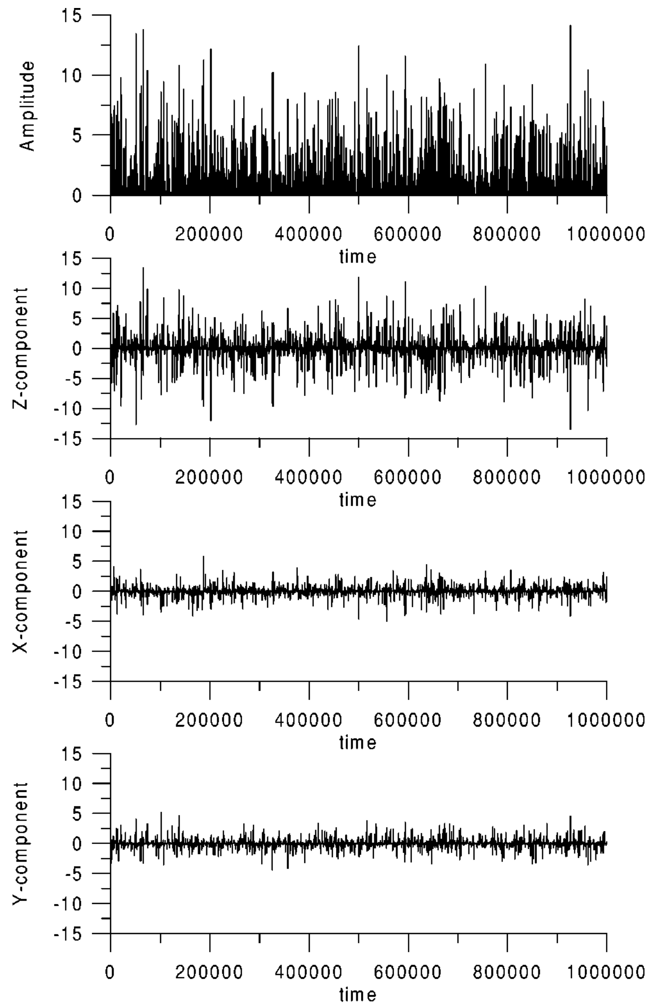

FIG. 5. Evolution of the mean magnetic field in the case of small values of H_0.

A. Choice of numerical values of parameters

At first view it could be thought that the model, containing many free parameters, would give any behavior of the system one might wish. But we never vary all the parameters; on the contrary we choose for most of them reasonable values, which are afterwards kept constant, after only checking that the results are stable with respect to small variations of these parameters. In any case, changing the parameters always carries a clear physical meaning, which can be discussed in relation with the system behavior (see below). Notwithstanding, not to arbitrarily restrict the model, we have written the equations in a general form.

We fix the parameters using a few simple principles. First, we get from the first simple model [33] information about the values that allow to obtain long-term symmetry breakings. The investigations of this previous model indeed

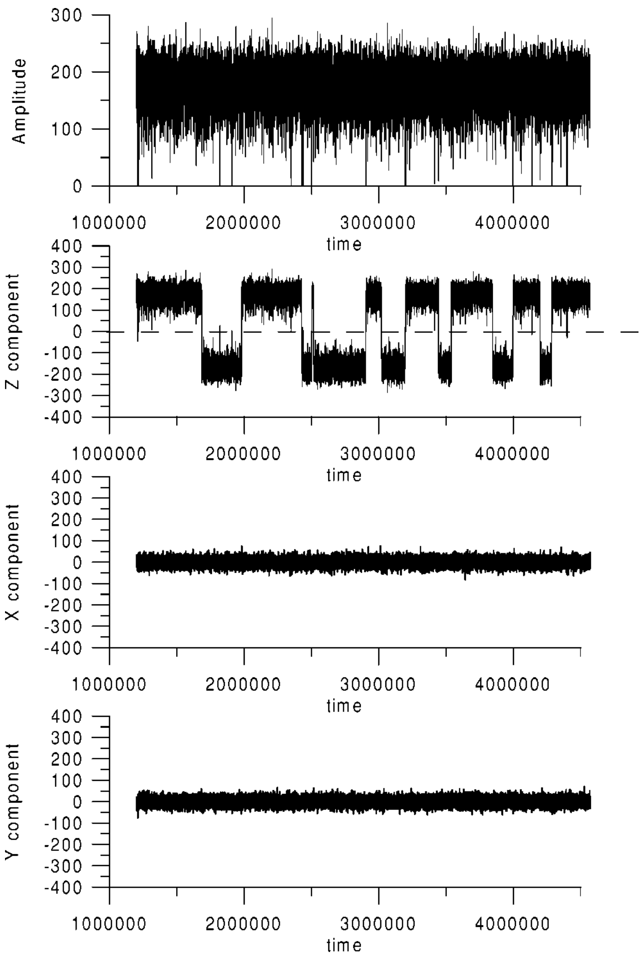

FIG. 6. Evolution of the mean magnetic field in the case of high values of H_0.

showed that, in order to obtain these long-term symmetry breakings, some conditions must be fulfilled: (a) the intensities of the inverse or direct cascades must not get too small; (b) the intensity of the appearance of the turbulence must not be too small or too large compared to the inverse of the lifetime of cyclones (nevertheless, for a fixed lifetime of cyclones, a range of two orders of magnitude is still admissible for the turbulence intensity). Coming to the present model, it also transpires that a nonzero influence coefficient *w* between the different domains [see Eq. (13)] is required. Taking a set of reasonable values of the system parameters, we describe however quite a general case of model behavior.

B. Phase transition through H_0

The value of H_0 governs the possibility to amplify the magnetic field using the energy of the turbulent helical motion when the intensity of the local magnetic field is close to zero. In this case indeed the main term in the square root of the right-hand side of Eq. (18) is $\sqrt{H_0|H_j|}$. When H_0 is small, the amplitude of the generated field is close to zero, and long chrons (intervals of constant polarity) do not appear in the evolution of the *Z* component of the field (Fig. 5).

When H_0 is large enough the *Z* component of the field is generally ten times larger than the two other components

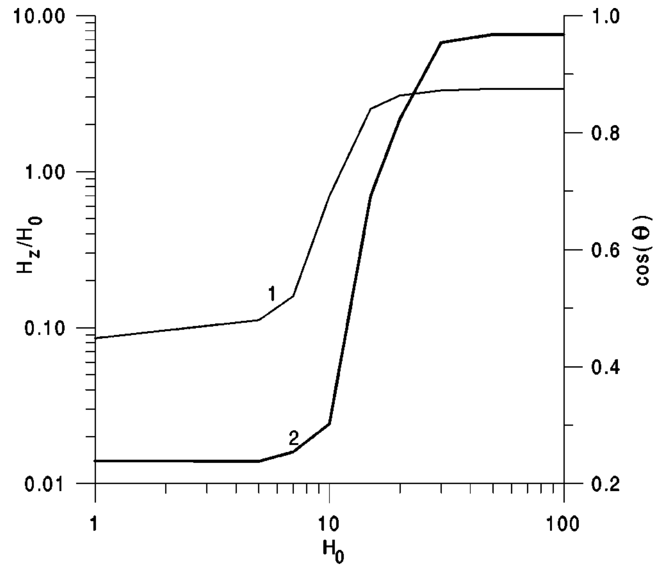

FIG. 7. The phase transition by the parameter H_0 of the mean relative amplitude of the *Z* component H_z/H_0 (curve 1) and the 5% quantile of $\cos(\theta)$ (curve 2).

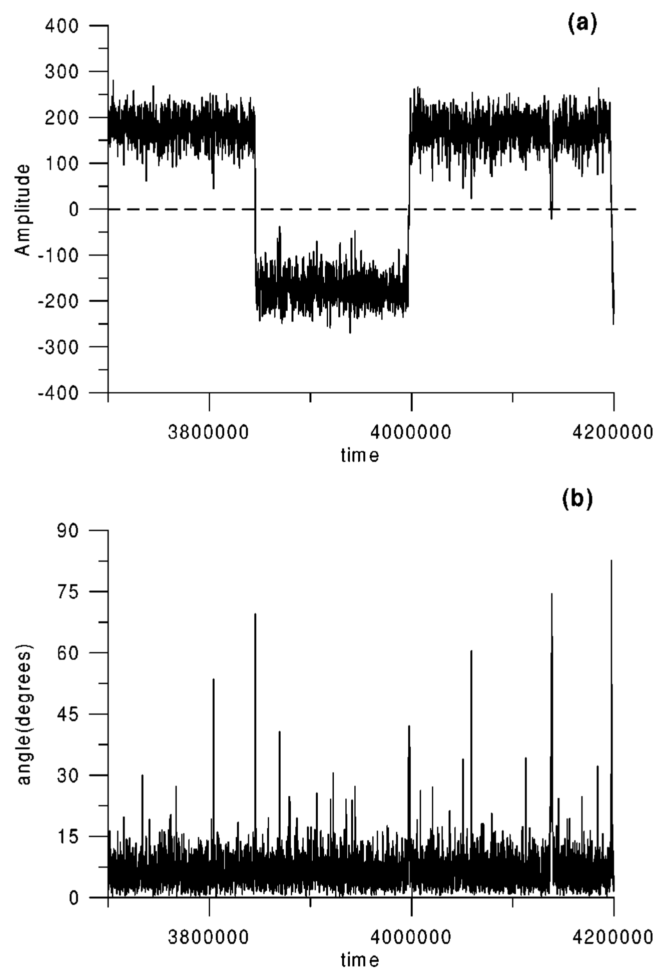

FIG. 8. Temporal evolution of the amplitude (a) of the mean magnetic field and the angle (b) between the vector of the field and the *Z* axis. High values of the angle correspond to the low absolute values of the amplitude.

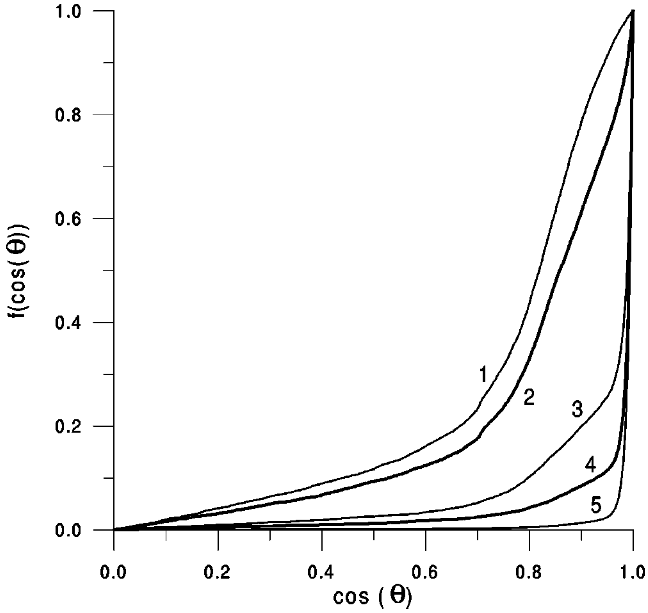

FIG. 9. Density functions of the distribution of angles between the mean magnetic field vector $\boldsymbol{H}$ and the Z axis for different values of the parameter H_0: $H_0=1$, curve 1; $H_0=10$, curve 2; $H_0=15$, curve 3; $H_0=20$, curve 4; $H_0=50$, curve 5.

(Fig. 6). The evolution of the Z component is then characterized by long-life intervals of constant polarity (chrons), with quick changes of polarity (reversals), (Fig. 6). A high intensity magnetic field can be generated from arbitrarily low initial values (as in the 2D model of [34]). So, the two basic properties of the real geomagnetic field evolution are successfully reproduced.

A phase transition from the first state (Fig. 5) to the second one (Fig. 6) occurs around a critical value H_0^{cr} of the parameter H_0. Let us consider the ratio $|H_z|/H_0$ as a function of H_0 where $|H_z|$ is the amplitude of the Z component of the mean magnetic field vector $\boldsymbol{H}$ defined above. It is clear [see graph (1) of Fig. 7] that H_z increases stepwise, by more than an order of magnitude when H_0 passes H_0^{cr}. In both phases, $H_0<H_0^{cr}$ as well as $H_0>H_0^{cr}$, the ratio $|H_z|/H_0$ is constant, which means that the amplitude of the resulting field is proportional to the energy transfer from the turbulent motion to the magnetic field (Fig. 7, curve 1).

Let us calculate the angle θ between the magnetic field vector $\boldsymbol{H}$ and its Z component $\boldsymbol{H}_z$:

$$\cos(\theta(t))=\frac{|H_z|}{\sqrt{H_x^2(t)+H_y^2(t)+H_z^2(t)}}. \qquad (20)$$

When the magnetic field of the model is axial dipolar, $\boldsymbol{H}$ reduces to its Z component; θ value is an estimate of the relative intensity of the non(axial)dipole component of the generated magnetic field.

Looking at the temporal evolution of the angle θ for large H_0 (Fig. 8), it appears that the generated field is close to its Z component inside a chron but may be quite far from it during a reversal or an excursion (Fig. 8). Inside a period of constant polarity the mean value of θ is about $7°$. The normalized distribution function for θ values tends toward a very sharply peaked function when H_0 grows (Fig. 9). Let us consider the 5% quantile of the distribution function. This quantity also presents a phase transition in the same interval the amplitude did (Fig. 7, curve 1). For overcritical values of H_0 the generated field is close to a dipolar field parallel to the Z axis for 95% of time (the probability of having angle $\theta<14°$ is larger than 0.95 for all $H_0>H_{cr}$).

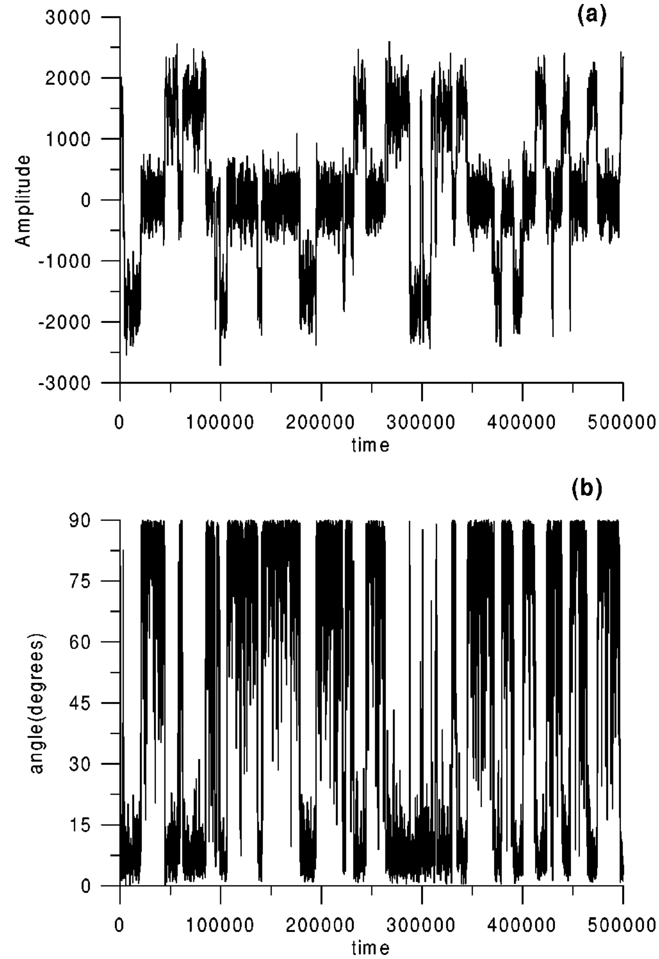

FIG. 10. Evolution of the amplitude (a) and the angle (b) of the mean magnetic field vector $\boldsymbol{H}$ in the case of isotropic turbulence.

VI. DISCUSSION

The present work is a step forward in our construction of a self-excited three-dimensional model of the geomagnetic field. It is well known that the magnetic field of the Earth is mainly axial dipolar. This axial symmetry was assumed in the construction of the first models [33,34], and conditions for long-life symmetry breaks (chrons) were obtained. In the present model we use a more general 3D construction and find that the axial symmetry introduced in the system of turbulent cyclones (linked with the Earth's rotation) results under certain conditions in an axial symmetry of the generated field.

The present model conserves the basic achievement of the previous ones [33,34]: it generates a magnetic field with long-life breaks of symmetry, reproducing the behavior of the magnetic field of the Earth during geological times.

The generalization from 2D to 3D model adds an additional necessary condition for long-life symmetry breaks (long constant polarity intervals) to occur: the transfer of kinetic energy from the system of cyclones to the magnetic field has to be strong enough. It is evident that in a dissipative self-excited system we have to assume some source of energy in order to obtain a nontrivial stationary behavior; transfer of kinetic energy from the motion of cyclones seems quite natural. The level of this transfer appears to be essential not only to the generation of a nonzero magnetic filed, but also to the polarity changes of its dipole component. Symmetry breaks in the 3D model are conditioned by a high enough activity of three basic processes: the direct cascade, the inverse cascade, and the energy transfer. The influence of the up and down cascades was derived in the 2D model; in the 3D model we obtain a phase transition governed by the intensity of the energy transfer from the system of turbulent cyclones to the generated magnetic field.

The present model has a schematic construction and describes the evolution of cyclones in a cylindrical layer rather than in a spherical volume. It allows, however, to estimate the influence of the model characteristics on the relationship between the analog axial dipole and nondipole components of the generated field. For example, it was shown that an isotropic turbulence (when the turbulence is isotropic at all levels even the highest one) leads to long-life periods of weak intensity of the Z component of the field (Fig. 10). As paleomagnetic data do not reveal such a behavior of the geomagnetic field, we have to assume an anisotropy of the turbulence in the model (the situation might be different for other planets). We intend to refine the construction of the model to be able to better simulate the geometric properties of the real geomagnetic field.

Modelization of the magnetic field of celestial bodies should not be limited to the Earth's case. The departures of the magnetic field of the giant planets from the field of an axial centered dipole can be quite large. Jupiter's field is rich in harmonies (multipoles); Uranus's dipole is strangely shifted from the planet center and its direction far from the rotation axis one; on the contrary Saturn's field is surprisingly close to the field of an axial centered dipole. Considering Earth-like planets, it is quite likely that Mercury has a dynamo functioning in its metallic core, while Mars and Venus have not. Mars magnetic field, which is known in some detail [43,44], is a fossil field like the Moon one. Recently the Galileo mission brought spectacular and unexpected results about the magnetic fields of Jupiter's satellites (e.g., [45–49]). Ganymede and Io have intrinsic magnetic fields (although Io's field might be generated by magnetoconvection in the Jovian background magnetic field, whereas an autoexcited dynamo in a metallic core is the preferred mechanism for Ganymede [48]. The variety of histories, compositions, and situations of the planets and moons feeds dynamo modeling with new constraints and questions. For example, it has been suggested that as a consequence of the ambient Jovian field the Ganymede dynamo cannot undergo reversals; this is easy to look at in the frame of the above model. All these observations should feed further reflections about the general considerations at the basis of the present model.

[1] T. Rikitake, Proc. Cambridge Philos. Soc. **54**, 89 (1958).
[2] P. Nozières, Phys. Earth Planet. Inter. **174**, 55 (1978).
[3] R. Hide, Nonlinear Proc. Geophys. **4**, 201 (1998).
[4] E.N. Parker, Astrophys. J. **122**, 293 (1955).
[5] S.I. Braginsky, Sov. Phys. JETP **20**, 726 (1964).
[6] F. Krause and K. H. Rädler, in *Ergebnisse des Plasmaphysik und der Gaselektronik*, edited by R. Rompe and M. Steenbeck (Akademie-Verlag, Berlin, 1, 1971), Bd. II.
[7] F. Krause and K. H. Rädler, *Mean-Field Magnetohydrodynamics and Dynamo Theory* (Pergamon Press, London, 1980).
[8] C.F. Barenghi, Geophys. Astrophys. Fluid Dyn. **60**, 211 (1991).
[9] R. Hollerbach, C.F. Barenghi, and C.A. Jones, Geophys. Astrophys. Fluid Dyn. **67**, 1 (1992).
[10] C.F. Barenghi, Geophys. Astrophys. Fluid Dyn. **67**, 27 (1992).
[11] S.I. Braginsky, Geomagn. Aeron. **18**, 225 (1978).
[12] S. I. Braginsky and P. H. Roberts, Geophys. Astrophys. Fluid Dyn. **38**, 327 (1987).
[13] D. Jault, Geophys. Astrophys. Fluid Dyn. **79**, 99 (1995).
[14] P. Hoyng, M.A.J.H. Ossendrijver, and D. Schmitt, Geophys. Astrophys. Fluid Dyn. **94**, 151 (2001).
[15] E. Dormy, J.P. Valet, and V. Courtillot, Geochem. Geophys. Geosyst. **1**, 62 (2000).
[16] G. Glatzmaier and P.H. Roberts, Phys. Earth Planet. Inter. **91**, 63 (1995).
[17] G. Glatzmaier, R. Coe, L. Hongre, and P.H. Roberts, Nature (London) **401**, 885 (1999).
[18] E. Grote, F.H. Busse, and A. Tilgner, Phys. Earth Planet. Inter. **117**, 259 (2000).
[19] A. Kageyama and T. Sato, Phys. Rev. E **55**, 4617 (1997).
[20] H. Kitauchi and S. Kida, Phys. Fluids **10**, 457 (1998).
[21] W. Kuang and J. Bloxham, Nature (London) **389**, 371 (1997).
[22] W. Kuang, and J. Bloxham, J. Comput. Phys. **153**, 51 (1999).
[23] P.H. Roberts and G. Glatzmaier, Geophys. Astrophys. Fluid Dyn. **94**, 47 (2001).
[24] F. Takahashi J. Katayama, M. Matsushima, and Y. Honkura, Phys. Earth Planet. Inter. **128**, 149 (2001).
[25] S. Braginsky, and V.P. Meytlis, Geophys. Astrophys. Fluid Dyn. **55**, 71 (1990).
[26] K. Zhang, and C. Jones, Geophys. Res. Lett. **24**, 2868 (1997).
[27] G. Sarson, and C. Jones, Phys. Earth Planet. Inter. **111**, 3 (1999).
[28] P. Olson and A. Aurnou, Nature (London) **402**, 170 (1999).
[29] P. Olson, U. Christensen, and G. Glastzmaier, J. Geophys. Res. [Planets] **104**, 10383 (1999).
[30] A. Sakuraba and M. Kono, Phys. Earth Planet. Inter. **111**, 105 (1999).
[31] F.H. Busse, E. Grote, and A. Tilgner, Stud. Geophys. Geod. **42**, 211 (1998).

[32] J.-L. Le Mouël, C.J. Allègre, and C. Narteau, Proc. Natl. Acad. Sci. U.S.A. **94**, 5510 (1997).
[33] E.M. Blanter, C. Narteau, M.G. Shnirman, and J.L. Le Mouël Phys. Rev. E **59**, 5112 (1999).
[34] C. Narteau, E. Blanter, J.-L. Le Mouël, M. Shnirman, and C.J. Allegre, Phys. Earth Planet. Inter. **120**, 271 (2000).
[35] A. J. Chorin and J. Marsden, *A Mathematical Introduction to Fluid Mechanics* (Springer, New York, 1993).
[36] A.J. Chorin, *Vorticity and Turbulence* (Springer, New York, 1994).
[37] P.S. Marcus, J. Fluid Mech. **215**, 393 (1990).
[38] P.H. Roberts, Mathematika **19**, 169 (1972).
[39] J. Marsden and A. Weinstein, Physica D **7**, 305 (1983).
[40] D. Montgomery, L. Phyllips, and M.L. Theobald, Phys. Rev. A **40**, 1515 (1989).
[41] J.P. Dahlburg, D. Montgomery, G.D. Doolen, and L. Turner, Phys. Rev. Lett. **57**, 428 (1986).
[42] X. Shan, D. Montgomery, and H. Chen, Phys. Rev. A **44**, 6800 (1991).
[43] M.H. Acuna, J.E.P. Connerney, P. Wasilewski, R.P. Lin, K.A. Anderson, C.W. Carlson, J. McFadden, D.W. Curtis, D. Mitchell, H. Reme, C. Mazelle, J.A. Sauvaud, C. d'Uston, A. Cros, J.L. Medale, S.J. Bauer, P. Cloutier, M. Mayhew, D. Winterhalter, and N.F. Ness, Science **279**, 1676 (1998).
[44] M.E. Purucker, D. Ravat, H. Frey, C. Voorhies, T. Sbaka, and M. Acuna, Geophys. Res. Lett. **27**, 2449 (2000).
[45] K.K. Khurana, M.G. Kivelson, C.T. Russell, R.J. Walker, and D.J. Southwood, Nature (London) **387**, 262 (1997).
[46] M.G. Kivelson, K.K. Khurana, F.V. Coroniti, S. Joy, C.T. Russell, R.J. Walker, J. Warnecke, L. Bennett, and C. Polanskey, Geophys. Res. Lett. **17**, 24 (1997).
[47] M.G. Kivelson, K.K. Khurana, S. Joy, C.T. Russell, R.J. Walker, and C. Polanskey, Science **276**, 1239 (1997).
[48] G. Schubert, K. Zhang, M.G. Kivelson, and J.D. Anderson, Nature (London) **384**, 544 (1996).
[49] J.D. Anderson, E.L. Lau, W.L. Sjogren, G. Schubert, and W.B. Moore, Nature (London) **387**, 264 (1997).